# Electrospun UV-cross-linked polyvinylpyrrolidone fibers modified with polycaprolactone/polyethersulfone microspheres for drug delivery

Adam Mirek, Marcin Grzeczkowicz, Habib Belaid, Aleksandra Bartkowiak, Fanny Barranger, Mahmoud Abid, Monika Wasyleczko, Maksym Pogorielov, Mikhael Bechelany, Dorota Lewińska

147 (2023) 213330

Contents lists available at ScienceDirect

Biomaterials Advances

journal homepage: www.journals.elsevier.com/materials-science-and-engineering-c

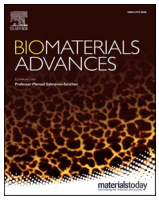

# Electrospun UV-cross-linked polyvinylpyrrolidone fibers modified with polycaprolactone/polyethersulfone microspheres for drug delivery

Adam Mirek [a,b,*], Marcin Grzeczkowicz [a], Habib Belaid [b], Aleksandra Bartkowiak [a], Fanny Barranger [b], Mahmoud Abid [b], Monika Wasyłeczko [a], Maksym Pogorielov [c,d], Mikhael Bechelany [b], Dorota Lewińska [a]

[a] Nalecz Institute of Biocybernetics and Biomedical Engineering, Polish Academy of Sciences, 4 Ks. Trojdena St., 02-109 Warsaw, Poland
[b] Institut Européen des Membranes, IEM, UMR 5635, Univ Montpellier, CNRS, ENSCM Place Eugène Bataillon, 34095 Montpellier cedex 5, France
[c] Sumy State University, Medical Institute, 40018 Sumy, Ukraine
[d] NanoPrime, 32-900 Dębica, Poland

ARTICLE INFO

*Keywords:*
Electrospinning
Microspheres
Suspension
Drug delivery
UV-cross-linking

ABSTRACT

Electrospun fibers, often used as drug delivery systems, have two drawbacks – in the first stage of their action a sudden active substance burst release occurs and they have a relatively small capacity for a drug. In this work the fibers are modified by the addition of drug-loaded microspheres acting as micro-containers for the drug and increasing the total drug capacity of the system. Its release from such a structure is slowed down by placing the microspheres inside the fibers so they are covered with an outer layer of fiber-forming polymer. The work presents a new method (microsphere suspension electrospinning) of obtaining polyvinylpyrrolidone fibers cross-linked with UV light modified with polycaprolactone/polyethersulphone microspheres loaded with active substance – rhodamine 640 as a marker or ampicillin as a drug example. The influence of UV-cross-linking time and the microspheres addition on the degradation, mechanical strength and transport properties of fibrous mats was investigated. The mats were insoluble in water, in some cases mechanically stronger, their drug capacity was increased and the burst effect was eliminated. The antibacterial properties of ampicillin-loaded mats were confirmed. The product of proposed suspension electrospinning process has application potential as a drug delivery system.

## 1. Introduction

Electrospun fibrous mats have been studied since the beginning of 20th century in the context of their potential use as controlled drug delivery systems. What makes them a very good candidate for this purpose are their great specific surface area, high porosity and structure similar to the extracellular matrix [1].

For the production of nano- and micro-thin fibers from a polymer solution or melt, the electrospinning method is used [2]. Synthetic polymers such as aliphatic polyesters e.g. poly(glycolic acid) (PGA), poly(lactic acid) (PLA), their copolymer (PLGA) and polycaprolactone (PCL), as well as hydrophilic polymers – poly(ethylene glycol) (PEG), poly(vinyl alcohol) (PVA) or polyvinylpyrrolidone (PVP) – are commonly used in the electrospinning process [3]. They have much greater strength, repeatability and processing flexibility than the natural ones, they can also help to avoid immunogenicity and pathogen transmission [4]. Polymers present in drug delivery systems should be appropriately selected for the nature of the drug used in them. For example, hydrophilic polymers (e.g. PVA) will be suitable for delivering water-soluble substances [5], while on the other hand, the use of hydrophobic polymers (e.g. PCL) delays the release of the substance, thus prolonging the performance of the system [6]. Electrospun PVP fibers are especially interesting in the context of drug delivery as they can be loaded with both types of drugs. Domokos et al. used fast dissolving properties of PVP to design orally disintegrating fibrous mats containing carvedilol – a poorly soluble in water active substance, while other systems were not able to provide its adequate therapeutic dose [7]. On the other side, Maciejewska et al. used PVP fibers to design antibacterial surfaces by functionalizing them with lysozyme – a hydrophilic antimicrobial enzyme. The fibers were electrospun with the addition of

* Corresponding author at: Nalecz Institute of Biocybernetics and Biomedical Engineering, Polish Academy of Sciences, 4 Ks. Trojdena St., 02-109 Warsaw, Poland.
*E-mail address:* amirek@ibib.waw.pl (A. Mirek).

https://doi.org/10.1016/j.bioadv.2023.213330
Received 18 November 2022; Received in revised form 24 January 2023; Accepted 2 February 2023
Available online 9 February 2023

benzophenone and cross-linked with ultraviolet light to reduce the solubility of the PVP (active substance carrier) in water [8]. PES-based ultrafine fibers also have the potential to be used as a drug carrier in drug delivery [9], e.g. for wound dressings [10].

Despite all their advantages that make electrospun fibers potentially applicable as controlled drug delivery systems, they also have some limitation. Microparticles and fibers designed as carriers share a common drawback – burst effect, a sudden initial uncontrolled release of the drug [11–13]. Once the system is placed in the release medium, there is a great ejection of the drug before the release rate reaches a stable profile [14]. This significantly increases the concentration of the drug in the initial phase of delivery and reduces the effective lifetime of the system as the amount of total burst-released substance might reach up to 55 % of the total release [15]. Burst release may result in unpredictable and undesirable effects, such as pharmacological risks, ineffective treatment, and economic losses [1]. Due to the fact that burst release is quick and short, most mathematical models for substance release ignore it. A solution to the burst release problem should therefore be sought in the appropriate modification of the drug delivery system.

Another limitation of classic electrospun fibrous mats is the relatively small capacity of such a system for an active substance. The electrospinning process usually takes several hours and produces fibers with nanometric diameters. The resulting mats are characterized by low weight due to the low output of the process (0.01–0.1 g/h, [16]) and high porosity (up to 99.2 %, [17]). The amounts of drugs that could be encapsulated in such a system are small (up to 10 mg), and the fibrous mat becomes useful only for low-dose applications [18]. In order to increase the capacity of the system for the drug, it is proposed, for example, to scale-up the electrospinning process [18], increase the fiber diameter [19] or modify fibers by in situ formation of microspheres within electrospun mats [20].

Various modifications of the electrospinning are used and they aim to improve the fibrous mats by giving additional properties to the fibers and removing the above-mentioned flaws of classical technique. Post-processing modifications can be applied to the electrospun fibers [21], but the process itself can also be modified, for example, by changing the shape of the electrospinning spinneret, replacing a simple single nozzle with coaxial [6], multiaxial [22] or side-by-side ones [23]. The result of such action is fibers with a complex multilayer structure of the core/shell or Janus type. This changes their transport properties for immobilized substances (e.g. the shell can slow drug release), mitigates the drawbacks relative to burst release and allows the development of mats made of polymers of two different types: hydrophilic and hydrophobic, which also broadens the application potential [24]. For example, Mo et al. conducted a coaxial electrospinning process with biologically active oil as a core and PCL as a shell which allowed the drug to be released for three days [25], and Zhao et al. developed PCL/Zein core-shell fibers loaded with metronidazole and prolonged the drug dissolution time from 18 h to 72 h [26].

Another modification is the emulsion electrospinning process in which the drug solution disperses in the form of micelles in the polymer solution to form a stable emulsion [27]. The advantage of this method is the minimized contact of the bioactive substance with an organic solvent that could damage it. Moreover, it does not require the use of coaxial electrospinning nozzle to form multilayer structures. Basar et al. fabricated the fibrous mat by emulsion electrospinning of a PCL/gelatin (O/W) emulsion with ketoprofen dispersed in oil phase. Such a system eliminated drug burst release effect and allowed it to be sustainably released for up to 4 days [28]. Shibata et al. improved the solubility of poorly water-soluble probucol (PBC) by dispersing it in PVA fibers electrospun from O/W emulsion where PBC was dissolved in ethyl acetate and PVA in water. Such a system enabled controlled release of poorly water-soluble drugs [29].

Another particularly interesting drug delivery system manufacturing method would be the combination of the electrospinning process with the production of drug-loaded microspheres. Such a solution would link the advantages of both techniques, eliminating their disadvantages. The use of microspheres as micro-containers for the active substance would increase the total volume of the system, while the fibers would allow it to maintain its integral structure, eliminating the risk of sphere migration. Such solutions are currently being developed mostly for the oil/water separation systems, such as the one proposed by Gao et al. [30]. They simultaneously electrospun polyvinylidene fluoride (PVDF) and electrospray $SiO_2$/PVDF microspheres to obtain the hybrid structure described above. The system combined the flexibility of the fibers with the hydrophobicity of the microspheres, which increased the oil adsorption capacity. In a similar way potential fibrous wound dressing materials can be designed [31,32]. Li et al. [31] proposed a multi-layered fibrous mat made by spraying the silk fibroin (SF)/chitosan (CS) microparticles onto the polycaprolactone (PCL)-polyvinyl alcohol (PVA) fibers. The system was found to have high encapsulation rate of bovine serum albumin (BSA) and good antibacterial effect. Gungor-Ozkerim et al. [32] created a “sandwich system” in which an electrosprayed growth factor-loaded gelatin microspheres layer was placed between two layers of electrospun fibers (PCL/PLA and PCL/gelatin). This system remained stable for at least 2 months, prevented microsphere migration, and the bioactive nature of growth factor was maintained. Another “sandwich system” was proposed by Nagiah et al. [33]. The results of their study show that a composite system consisting of doxycycline hyclate-loaded poly (vinyl alcohol) microspheres sandwiched between poly (3-hydroxybutyric acid) electrospun fibers has an initial burst release despite the multi-layered system. It is noteworthy that each of the above methods assumes the formation of microspheres and fibers independently, with subsequent combination at the collector. This results in the entanglement of microspheres within the fiber network, forming mixed systems. The microspheres are not immobilized within the fiber structure, covered with an outer polymer layer. Such a structure could potentially be achieved through a microsphere suspension electrospinning, which is currently an under-explored method. The authors of the present study have identified a limited number of investigations that delve into the topic of the utilization of this technique for the production of potential drug delivery systems. Xu et al. [34] developed a biodegradable drug delivery system (electrospun poly (l-lactic acid) fiber mats loaded with chitosan microspheres) using a suspension electrospinning method. In vitro dual release showed short-lived release of bovine serum albumin, but long-lasting release of benzoins in all dual drug release systems. The diameters of both the microspheres and fibers were observed to range between 1 and 3 μm.

The aim of the presented work was to develop a new potential drug delivery system based on water-insoluble polyvinylpyrrolidone fibers modified with polycaprolactone (or polyethersulfone) microspheres manufactured using a suspension electrospinning process. A series of actions were undertaken to achieve the research objective. Firstly, it was decided to modify PVP fibers with microspheres of diameters 10–20 times greater than fiber diameters, used as drug carriers. The intention was to increase the capacity of the entire system for the active ingredient and to eliminate the burst effect that normally may occur when microspheres or electrospun fibers are used as individual drug systems. The microspheres used for modification were prepared by a method combining pulsed voltage electrospray and wet phase inversion techniques, as detailed in a previous study [35]. Subsequently, in order to stabilize the complex suspension electrospinning process, it was decided to supply the electric charge in a pulsed manner (pulsed voltage – PV). This unconventional method introduces two additional electric process parameters – the duration of electric pulses and their frequency, which significantly improves the ability to control the electrospinning process [36,37] and in consequence the properties of the obtained fibers. Finally, to improve the stability of the modified fibrous mats and prevent their dissolution in water, crosslinking of PVP with ultraviolet light using benzophenone as a photoinitiator was evaluated as a potential solution. In accordance with the established assumptions, such a novel modified electrospun drug delivery system would maintain its

therapeutic potential in an aqueous environment and release the drug in a controlled, prolonged manner which would improve its effectiveness. To fully understand the properties and capabilities of the proposed system, a comprehensive set of experiments were conducted, including assessments of degradation in water and ethanol, evaluations of mechanical characteristics, spectrophotometric studies of marker content and release, and examination of the antibacterial properties of the drug-loaded mats.

## 2. Materials and methods

### 2.1. Materials

Poly(vinyl pyrrolidone) (PVP, $M_W$ = 1300 kDa, CAS Number: 9003-39-8) was purchased from Acros Organics (Belgium), polycaprolactone (PCL, $M_W$ = 70 kDa, CAS Number: 24980–41–4) was purchased from Scientific Polymer Products (USA) and polyethersulfone (PES, $M_W$ = 42 kDa, Ultrason E2020) from BASF (Germany). Dimethylformamide (DMF, Chempur, Poland, CAS Number: 68–12–2, ≥99 %) and *N*-methyl-2-pyrrolidone (NMP, Chempur, Poland, CAS Number: 872–50–4, ≥98 %) were used as solvents for the polymers (PCL and PES respectively). Ethanol (EtOH, Polmos, Poland, ≥95 %) was used as a solvent for PVP and a PCL/PES non-solvent to induce phase separation in a precipitation bath. Benzophenone (BP, Sigma Aldrich, CAS Number: 119-61-9, ≥99 %) was used as a fiber UV-cross-linking photoinitiator. Hanks' Balanced Salt solution (HBSS) was used as a medium for cross-linked PVP mat degradation tests. The ingredients were purchased from POCH (Poland): sodium chloride (NaCl, CAS Number: 7647-14-5, ≥99.5 %), potassium chloride (KCl, CAS Number: 7447-40-7, ≥99.5 %), sodium phosphate dibasic ($Na_2HPO_4$, CAS Number: 7558-79-4, ≥98 %), potassium phosphate monobasic ($KH_2PO_4$, CAS Number: 7778-77-0, ≥99.5 %), calcium chloride ($CaCl_2$, CAS Number: 10043-52-4, ≥96 %), magnesium sulfate heptahydrate ($MgSO_4{\cdot}7H_2O$, CAS Number: 10034-99-8, ≥99 %), sodium bicarbonate ($NaHCO_3$, CAS Number: 144–55-8, ≥99 %), glucose (CAS Number: 50–99-7, ≥99.5 %), phenol (CAS Number, 108-95-2, ≥99 %). Rhodamine 640 perchlorate ($M_W$ = 591.05 Da, Exciton, USA, CAS Number: 72102–91–1) was used as a drug marker. Ampicillin sodium salt antibiotic (CAS Number: 69–52–3) was obtained from A&A Biotechnology (Poland). The non-pathogenic Gram positive *Staphylococcus aureus* and Gram negative *Escherichia coli* bacteria (K12 DSM 423, from DSMZ, Germany) were chosen as a model microorganism. The culture medium was a Tryptone Salt Broth (TSB, Sigma Aldrich). The chemicals were used without further purification. All solutions were prepared with MilliQ water (with a resistivity of 18.2 MΩ·cm; Millipore, USA).

### 2.2. Microsphere preparation

Microspheres were prepared using a method combining pulsed voltage electrospray and wet phase inversion techniques which was elaborated in our Laboratory [35]. The process setup scheme is shown in Fig. 1A. In this method, the polymer solution (PCL in DMF or PES in NMP) is pressed through a metal nozzle connected to a high pulsed voltage. At the nozzle outlet, electrospray process occurs and microdroplets are formed. Then, they are collected in a well-stirred precipitation bath filled with a non-solvent of the polymer. In this bath, wet phase inversion process takes place according to the Gibbs phase rule and solidified polymer microspheres are formed. The method can be modified by adding various substances (e.g. drug) to the polymer solution and bath and hence immobilizing them inside the microspheres.

The following polymer solutions were prepared to manufacture microspheres: 15 % PCL in DMF and 15 % PES in NMP. In order to prepare microspheres with an immobilized rhodamine or ampicillin, polymer solutions containing 0.57 mg/g (marker mass/polymer mass) of marker/ampicillin were used. The active substance was also added to the precipitation bath in the amount of 0.1 mg/mL. The values of the electrical parameters in the study were set as follows – electrical voltage $U$ = 8 kV, pulse frequency $f$ = 60 Hz, pulse duration $\tau$ = 6 ms. The polymer solution was delivered to the nozzle at a flow rate of 1.5 mL/h. After the formation of microspheres, the collecting bath content was transferred to a falcon and centrifuged in order to remove the excess ethanol off above the sedimented microspheres. Finally, they were dried at room temperature for several days to take the powder form ready for weighing and use in the next part of work. The temperature did not exceed 25 °C and a humidity – 40 % during whole procedure. The average diameters of the obtained microspheres were 14.38 ± 6.28 μm for PCL and 6.20 ± 2.43 μm for PES.

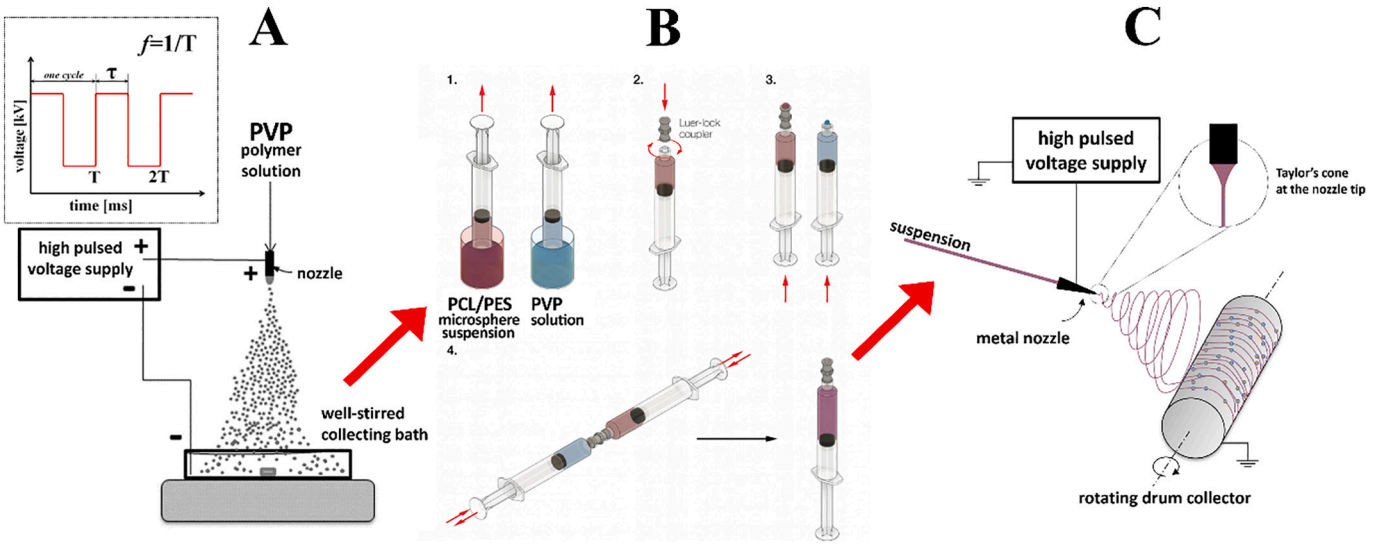


**Fig. 1.** The consecutive stages of the process of the manufacturing of polymer fibrous mats modified with microspheres. (A) Scheme of the process of microspheres production using the method developed previously by the authors [35]. (B) Scheme of mixing microspheres with polymer solution to obtain a suspension of microspheres by the syringe coupler method proposed by Allevi, Inc. [38], image used with permission from Allevi. (C) Scheme of the microsphere suspension electrospinning process on a drum collector.

### 2.3. Suspension electrospinning

The syringe coupler method (Fig. 1B) was used to prepare the suspension for electrospinning. 5.4 mL of the PVP solution in ethanol at the concentration of 18.5 % with the addition of benzophenone at the concentration of 3.75 % was placed in one syringe. 4.6 mL of the suspension of PCL or PES microspheres in the amounts of 50–300 mg in ethanol was placed in the other syringe. The syringes were connected using a syringe coupler and their contents mixed by moving the plungers back and forth approximately 40–50 times. In this way, a suspension of microspheres with a concentrations of 5–30 mg/mL in a PVP solution with a concentration of 10 % in ethanol with the addition of BP in an amount of 2 % was obtained.

The fibrous mats without the addition of microspheres were also electrospun for degradation tests and comparison purposes, using a PVP solution with a concentration of 10 % in ethanol with the addition of BP (2 %).

The electrospinning process was performed using a setup showed in the Fig. 1C. It is comprised of a custom-built high voltage pulse generator, an infusion pump with a syringe filled with microspheres/polymer suspension, a steel nozzle (external diameter of 0.9 mm), and a rotating grounded aluminum drum collector (diameter 47.5 mm, width 150 mm) placed 15 cm from the nozzle tip. The flow rate of the electrospun suspension was set as 0.6 mL/h. To avoid clogging the nozzle, the fibers were electrospun using pulsed voltage (PV) with electrical parameters – voltage U = 8 kV, pulse frequency f = 100 Hz, pulse duration $\tau$ = 8 ms. The geometric shapes of the suspension at the end of the nozzle were recorded. The resulting fibrous mats were being collected on a drum collector (rotation speed 120 $min^{-1}$) for 6 h each, the total volume of the electrospun solution was thus approximately 3.6 mL. After the process was completed, the polymer mats were cross-linked using ultraviolet light (365 nm). They were UV-exposed on each side for 5 min, 15 min and 60 min and marked 2 × 5 min, 2 × 15 min, and 2 × 60 min, respectively.

### 2.4. Characterization of the electrospun mats

The morphology of the polymer fibers with microspheres was examined using digital microscope (Keyence, VHX-7000) and SEM – the samples were coated with 10 nm thick gold layer for it. The microspheres in the mats were counted and their quantity *N* was determined as microspheres/$mm^2$. The diameters of 100–200 randomly selected fibers on a set of approximately 5–6 images for each condition were measured using the microscope software and their average values *d* were calculated. The statistical analysis of the obtained data was performed by determining the standard deviation from the mean value (*SD*) and the coefficient of variation (VC), which is represented as a percentage of the ratio of *SD* to the mean diameter (*d*).

The degradation of the UV-cross-linked fibrous mats was investigated. Samples 2 × 5 min, 2 × 15 min and 2 × 60 min of 5–6 mg weight were placed in 10 mL of HBSS solution each. The HBSS solution was prepared according to the method given in literature [39]. It was used because of its similar composition to blood plasma [40]. The degradation was carried out at 37 °C in a laboratory cradle with a rocking speed of 10 cycles per minute. The influence of degradation was assessed using scanning electron microscopy (SEM, Hitachi TM-1000) pictures of the mats made before the process, after 6 h and after 24 h. The diameters of 50 randomly selected fibers after degradation were measured and their average values were calculated. In addition, a long-term degradation test was performed – a 2 × 60 min mat sample was placed in ethanol for 2 months, and then analyzed by SEM.

The mechanical properties of the fibrous mats were tested using Zwick Roell ProLine tensile testing machine (Germany) with a solid fixture – tensile strength and elongation at break were measured. Mats were carefully peeled off from the aluminum collector surface and cut into 50 × 10 mm strips with the thickness about 0.3 mm. The speed of tensile testing was 0.2 mm/s. Five specimens were tested for each sample type. The mean values of mechanical parameters were determined as well as the statistical analysis of the obtained data was conducted, including the determination of the standard deviation (SD) and the coefficient of variation (VC) expressed as a percentage ratio of SD to the mean value. The measurement setup is shown in Fig. SI1 (supporting information). Microsoft Excel, OriginPro and GraphPad Prism software were used to perform all calculations and analyses as well as to plot the graphs.

### 2.5. Rhodamine immobilization in the mats

In order to check how the addition of microspheres increases the capacity of the system for the active substance compared to fibers without the addition, four types of electrospun fibrous mats with a marker (rhodamine) were made: without microspheres with the content of rhodamine in the electrospinning solution 0.0575 mg/mL, with rhodamine-loaded PCL microspheres at 10 mg/mL or 20 mg/mL and with rhodamine-loaded PES microspheres at 20 mg/mL. In each case, the microspheres which were used, were made by the technique described above, from a solution containing 0.1 mg/mL of rhodamine. They were distributed in an electrospinning solution with a rhodamine content of 0.0575 mg/mL. Two samples were taken from each mat and UV-cross-linked 2 × 5 min and 2 × 15 min. Then 4.4–6.7 mg of material were taken from each of them and placed in 2.40–3.65 mL of RO water, the volume of which was adjusted so that the ratio of mat weight to this volume remained the same in each case (5.5 mg/3 mL). Rhodamine was released from the mat samples for 4 h using a lab shaker to agitate the system. After this time, the rhodamine concentration in each of the solutions was determined using a spectrophometric method (light wavelength: 574 nm). The mean values of rhodamine concentration were determined based on three tests, the standard deviation (SD) and the coefficient of variation (VC) were determined as a part of statistical analysis.

### 2.6. Study of the rhodamine transport properties of the mats

For the study of rhodamine release profile, three types of mats were produced – with marker and no microspheres (PVP_Rod), with marker-loaded PCL microspheres (PVP_PCL/Rod) and with marker-loaded PES microspheres (PVP_PES/Rod). The amount of rhodamine was selected, and the mats were suitably prepared so that marker content in each mat (15 × 15 cm, fibers and microspheres) was ~0.6 mg. After the process was completed, the polymer mats were cross-linked using ultraviolet light for 2 × 5 min and 2 × 15 min. The kinetics of rhodamine release from fibrous mats was determined using a flow spectrophometric method (light wavelength: 574 nm). Two round samples with diameter of 14 mm and thickness 150–300 μm each and overall weight 5.0–6.5 mg were cut from each mat and placed together in a well-stirred glass container with 2.7–3.5 mL ($V_0$) of deionized water, the volume did not change during the experiment. Absorbance measurements were made every 2 min for the first 2 h, every 10 min for the next 1 h, every 30 min for the next 2 h, and after 6, 7 and 24 h after starting the experiment. The mean value of absorbance was determined based on a series of three experiments per case. The rhodamine release profiles were plotted on graphs. The transport properties of the tested mats towards rhodamine were investigated. They can be described with a linear function fitted to the plotted experimental points in the first stage of the substance release. The linear fitting in OriginPro software gave the equation of the line describing each case $y = \alpha x$, where α defines the slope of the line and thus the substance release rate.

The shape of the marker release curves from microsphere-loaded mats allows the use of a more complex Radcliff model [41] for the mathematical description of the release profile. According to Radcliff, mass transfer between two phases can be generally described by Eq. (1):

$$V_0\frac{dC}{dt} = -hA(C - C_S) \quad (1)$$

where: $C$ (mg/mL) – the marker concentration in liquid outside the material (mats), $C_S$ – concentration of the marker inside the material (mats) close to interphase boundary, $A$ ($cm^2$) – interface surface area (total external surface area of the mats), $V_0$ ($cm^3$) – the volume of liquid outside the material (mats). The symbol $h$ (cm/min) designated the mass transfer coefficient which describes the substance release rate in the first release period before equilibrium is reached.

Taking into account the specificity of the electrospun mats, it can be assumed that their entire volume is available for the marker, the marker does not reabsorb inside the material and initial marker concentration in solution is equal to 0, Eq. (1) can be supplemented with the mass conservation Eq. (2):

$$\frac{d(V_0C + V_CC_S)}{dt} = 0 \quad (2)$$

where $V_c$ ($cm^3$) – the volume of fibers.

After solving Eq. (1) in this case, the change in the marker concentration in the surrounding solution is described by the Eq. (3) [42]:

$$C = C_{eq}\left(1 - e^{-hA\left(\frac{1}{V_0}+\frac{1}{V_C}\right)\bullet t}\right) \quad (3)$$

where: $C_{eq}$ (mg/mL) – equilibrium marker concentration, $t$ (min) – time (independent variable).

Mathematical modeling of the process of rhodamine release from fibrous mats containing microspheres was performed with OriginPro software. The curves were fitted to the data using the exponential fit with the *BoxLucas1* mathematical model available in the program library which is described by Eq. (4):

$$y = a \bullet \left(1 - e^{-bx}\right) \quad (4)$$

where: $a$, $b$ – Origin model equation coefficients and $x$ – independent variable.

After the comparison of the power exponents in Eqs. (3) and (4), the following relationship is obtained:

$$-hA\left(\frac{1}{V_0}+\frac{1}{V_c}\right) \bullet t = -b \bullet x \quad (5)$$

Finally, after solving the Eq. (5), assuming that $x = t$ (variable), the expression for the coefficient $h$ is as follows:

$$h = \frac{b}{A\left(\frac{1}{V_0}+\frac{1}{V_c}\right)} \quad (6)$$

In order to determine the coefficient h, the values of $b$, $A$, $V_0$ and $V_C$ must be determined.

Value of parameter $b$ was generated by the *OriginPro* software using *BoxLucas1* mathematical model described by Eq. (4). An example of fitting the exponential model curve to the experimental results in the form of a graph with data generated by the software is shown in Fig. SI2A, while the geometric interpretation of model parameters $a$ and $b$ in Fig. SI2B (supporting information). The graphical interpretation of the $h$ coefficient (associated with the parameter $b$) is the first derivative of the *BoxLucas1* function, while the value of the parameter $a$ corresponds to the equilibrium concentration $C_{eq}$ determined by the software. Interface surface area $A$ was determined for each sample using nitrogen adsorption–desorption isotherms (BET analysis) at liquid nitrogen temperature using Micromeritics ASAP 2010 equipment (degassing conditions: 30 °C, 24 h). Solution volume $V_0$ is selected for each sample and varies from 2.7 to 3.5 mL. Sample volume $V_c$ was estimated from the dimensions of the sample (cylinder of 14 mm in diameter and 0.2 mm in height on average) and its value equals approximately 0.031 $cm^3$. The standard deviation (SD) and the coefficient of variation (VC) for $h$ values were determined as a part of statistical analysis.

### 2.7. Antibacterial activity of the electrospun mats loaded with ampicillin

For the antibacterial tests three types of fibrous mats were prepared – with no ampicillin, with ampicillin-loaded PCL microspheres and with ampicillin-loaded PES microspheres. Two types of mats were tested – cross-linked for 2 × 5 min and 2 × 15 min. The UV cross-linking provided sample sterilization too.

The antibacterial activity of ampicillin-loaded mats was examined against *Staphylococcus aureus* (*S. aureus*, Gram positive) and *Escherichia coli* (*E. coli*, Gram negative) bacteria. Fresh Tryptone Salt Broth (TSB) medium was inoculated by bacteria and incubated overnight at 37 °C in aerobic conditions. Bacterial cells were harvested by centrifugation and resuspended in a TSB when the stationary phase was reached. The bacterial suspension was then diluted to adjust the optical density at 620 nm ($OD_{600}$) to 0.75 ± 0.01 for *S. aureus* and 0.80 ± 0.01 for *E. coli*. Mueller-Hinton agar (GMH) plates were prepared by adding microbiological agar (15 g/L) to PBS medium; rectangular dishes were used. GMH agar plates were inoculated individually with 1 mL of *S. aureus* or *E. coli* suspension. Immediately after, the mat samples (10 × 10 mm) were put onto the plates to check their ability to prevent bacterial growth. Each sample contained approximately 0.003 mg of ampicillin. The plates were incubated at 37 °C in aerobic conditions overnight to allow the form a bacterial biofilm. To show inhibited bacterial growth (the clear zones), plates were pictured with a camera. The results of the study, which were obtained through three replicates of each test condition, were then quantified by measuring the diameter of the inhibition zone and calculating its area. The average values, along with standard deviations and coefficients of variation, are presented in a bar chart for ease of interpretation.

## 3. Results and discussion

### 3.1. Influence of UV-cross-linking on the fibrous mat degradation

The influence of the UV-cross-linking time of fibrous mats on their structure and properties was investigated. Fig. 2 shows SEM pictures of mats at successive stages of degradation in HBSS. Fig. 3 shows the change in fiber diameter during degradation.

The fibrous mat retains its structure regardless of the UV-cross-linking time (Fig. 2A, D, G), and the fiber diameters do not change ("0" bars in Fig. 3). The addition of BP and the UV-cross-linking process do not influence the smoothness of the fibers neither which was previously confirmed by Maciejewska et al. [8]. The mat UV-cross-linked for 2 × 5 min shows the phenomenon of formation of an outer layer ("skin") on the surface after 6 h (Fig. 2B) and 24 h of degradation (Fig. 2C). This "skin" is formed on both sides of the mat (Fig. 2J). Such a skin is not formed during the degradation of the UV-cross-linked mat 2 × 15 min and 2 × 60 min. In both of these cases, the fibers fuse with each other, creating irregular structures – in the case of the 2 × 15 min mat, this effect is visible after 24 h (Fig. 2F), and in the case of the 2 × 60 min mat also after 24 h (Fig. 2I) – marked in red circles.

UV-cross-linking of PVP fibers with benzophenone addition prevents their degradation not only in the aquatic environment. The mat UV-cross-linked for 2 × 60 min was placed in ethanol for 2 months. The degradation effect is different than in the case of the aqueous solution, there is no "skin". The fibers are highly swelled, the mat lost its original structure of individual, randomly arranged fibers, which stuck together, but did not completely degrade (Fig. 2K). This seems particularly relevant in view of the potential use of such fibers as a drug delivery system, because it opens the possibility of sterilizing the material using ethyl alcohol instead of, for example, UV radiation, which would alter the properties of the fibers through UV-cross-linking.

With the degradation time, the mean diameters of the UV-cross-

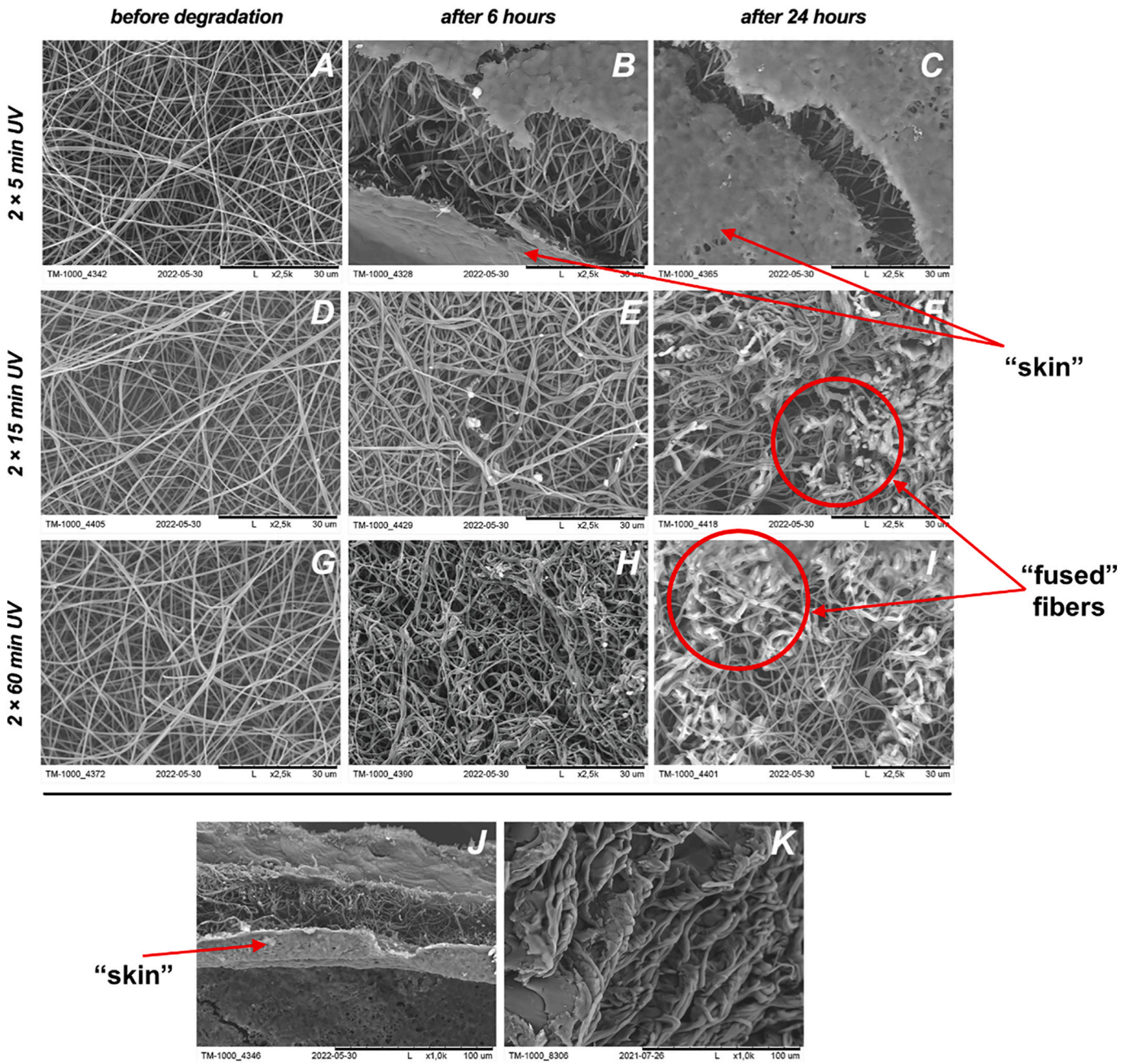


**Fig. 2.** Exemplary SEM pictures of the UV-cross-linked PVP fibers (without the addition of microspheres) at various stages of degradation in (A–J) HBSS or (K) ethanol. (A–C) cross-linking 2 × 5 min: (A) before degradation, (B) after 6 h of degradation; (C) after 24 h. (D–F) cross-linking 2 × 15 min: (D) before degradation, (E) after 6 h of degradation; (F) after 24 h. (G-I) cross-linking 2 × 60 min: (G) before degradation, (H) after 6 h of degradation; (I) after 24 h. (J) cross-linking 2 × 5 min after 24 h of degradation, side section. (K) cross-linking 2 × 60 min after 2 months of degradation in ethanol.

linked fibers for 2 × 5 min and 2 × 15 min increase from 0.5 to 0.7 μm, while UV-cross-linked fibers for 2 × 60 min do not change diameter. Furthermore, it can be observed that the uniformity of the fibers decreases, as evidenced by an increase in the coefficient of variation of diameter, which change from 13 % for non-cross-linked fibers up to 27 % for the cross-linked ones.

This effect is most likely due to the swelling of the fibers, which is more difficult in the case of a highly UV-cross-linked fibrous mat (2 × 60 min). This property of UV-cross-linked PVP fibers is not unexpected considering the fact that PVP is used, among others, to produce electrospun fibrous hydrogels capable of absorbing high levels of water or media uptake, spanning from 400 wt% to 1400 wt% [43].

The degradation process of the tested UV-cross-linked fibers can be divided into several stages. In the first stage, the slow swelling of the UV-cross-linked fibers leads to an increase in their diameters. In the second stage, the fibers begin to dissolve and lose their original structure (they join and fuse to form homogeneous structures on the surface, which may eventually take the form of a layer – "skin"). Such a layer, after drying, breaks, revealing non-degraded fibers inside (third stage).

The degradability of the UV-cross-linked PVP fibrous mats can be controlled by selecting the cross-linking time or the appropriate amount of benzophenone, as well as the thickness of the mat and the fiber diameters [44]. Such a system requires optimization with regard to its potential application.

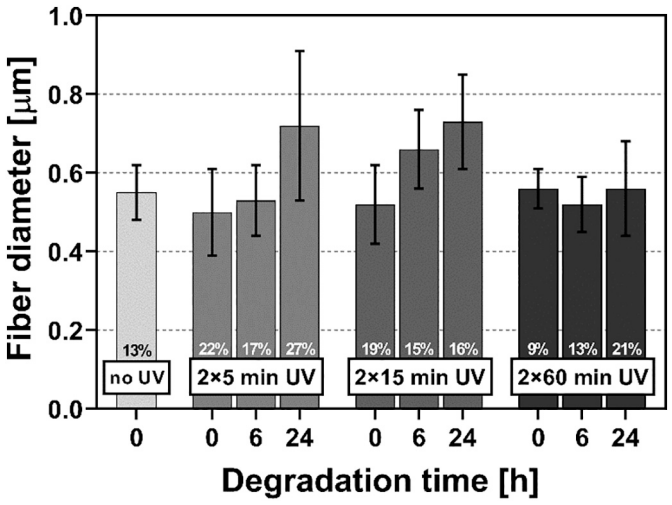


**Fig. 3.** Mean diameters of the UV-cross-linked PVP fibers (without the addition of microspheres) at various stages of degradation. The coefficient of variations of fiber mean diameter is indicated on each corresponding bar.

### 3.2. Microsphere suspension electrospinning feasibility

The feasibility of electrospinning of the PVP solution with PCL microspheres suspended was tested by checking their different contents in the initial suspension until a value was reached at which electrospinning did not proceed. The study was carried out only with PCL microspheres. Non-cross-linked mats were used in the research. Fig. 4 presents SEM pictures of fibers depending on the content of microspheres in the suspension $Q$ [mg/mL] with the estimated content of microspheres in the mats $N$ [$mm^{-2}$] and fiber mean diameter $d$ [μm].

Electrospinning of a suspension of PCL microspheres in a PVP solution is possible, but there is a limitation in the amount of microspheres at which such a mixture is no longer electrospinnable. In the present work, it was determined as >20 mg of microspheres per 1 mL of solution. Below this value, for the microspheres contents of 5 mg/mL and 10 mg/mL, electrospinning is stable and the fibers with microspheres (Fig. 4A–B) are collected. For the microspheres content of 20 mg/mL, the resulting mat contains the most microspheres, according to predictions (Fig. 4C). The 30 mg/mL microspheres content turned out to be too high – fibers are not formed on the collector. Solvent evaporates too quickly, polymer clogs the nozzle in the case. It was therefore decided to conduct electrospinning with a microspheres content of 20 mg/mL because of the high content of microspheres in the mat and that potentially increases its volume, which is the main goal of our work.

The microspheres in the fibers are mostly centrally located and covered with a polymer (like in core/shell fiber type), as can be seen in the SEM photos in Fig. 4D–E, and confirmed by optical microscope studies, due to the fact that PVP fibers are transparent (Fig. 4F). This fiber structure (microspheres covered by the outer polymer layer) is desirable in drug delivery systems as it can limit the burst effect [22]. It was noticed that the amount of microspheres added did not affect the diameter of the fibers.

### 3.3. Mechanical properties

Mechanical properties of mats depending on the content of microspheres, their type and cross-linking time were investigated. The results in the form of graphs showing tensile strength and elongation at break are summarized in Fig. 5.

UV-cross-linking improves the mechanical strength of fibers without microspheres (red bars, Fig. 5) – tensile strength is increased from about 0.2 MPa to 0.25 MPa, while elongation at break from 10 % up to 25–35 % (depending on cross-linking time). Interestingly, the longer the cross-linking time, the lower the fiber strength for both types of fibers – those without the addition of microspheres and those containing PCL or PES microspheres. The values of the variation coefficients of the relevant parameters serve as an indication of the accuracy of the measurement method employed, and if they surpass 10–15 %, they can be understood as an indication of the inhomogeneity of the fibrous mats.

The phenomenon of improving the mechanical strength of PVP fibers UV-cross-linked with benzophenone was also noted by Maciejewska et al. [8] who explained it by the cross-linking mechanism. Benzophenone is a photoactive molecule which, after absorption of a UV photon with a wavelength of 250–365 nm, is excited and produces a ketyl

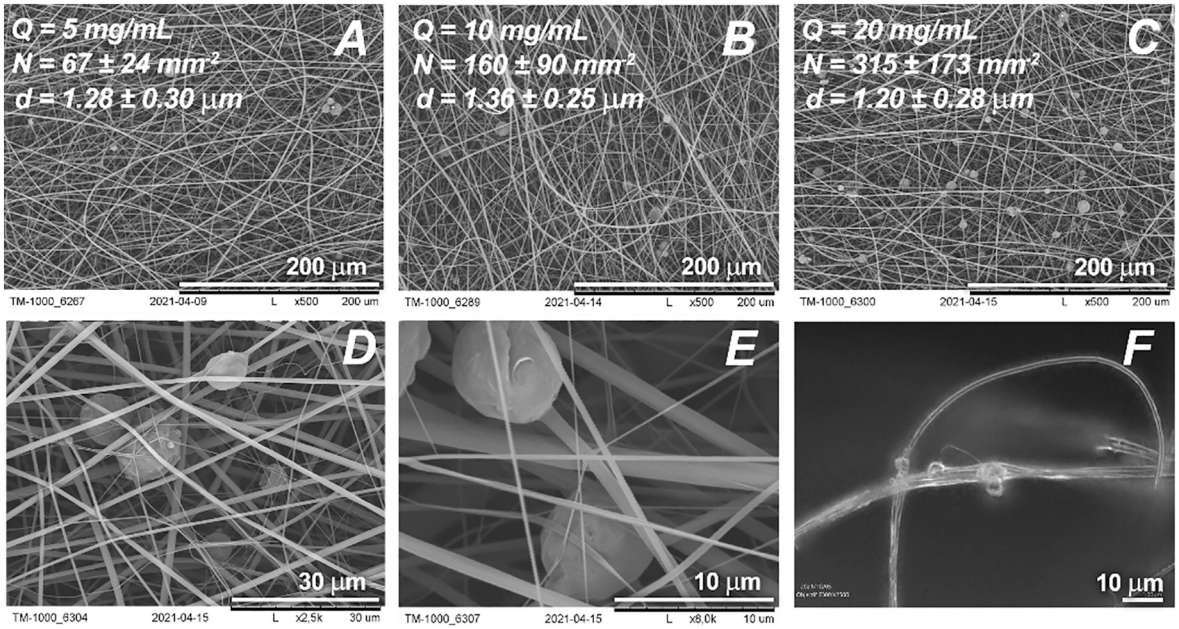


**Fig. 4.** (A–C) Exemplary SEM pictures (magnification 500×) of PCL microsphere-loaded PVP fibers depending on the content of microspheres in the suspension Q [mg/mL]: (A) 5 mg/mL, (B) 10 mg/mL, (C) 20 mg/mL. (D–E) Exemplary SEM pictures of fibers with PCL microspheres, magnification (D) 2500×, (E) 8000×. (F) Exemplary optical microscope picture of PVP fibers with PCL microspheres, magnification 2500×.

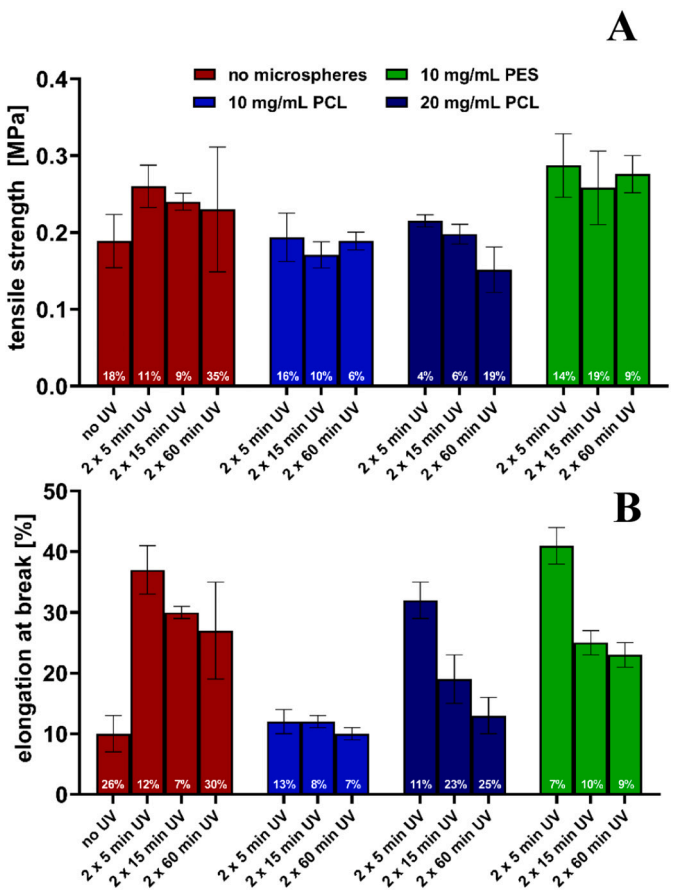


**Fig. 5.** Mechanical properties of UV-cross-linked microsphere-loaded PVP fibrous mats depending on the quantity and type of microspheres and cross-linking time: (A) tensile strength, (B) elongation at break. The coefficient of variations of mechanical parameters is indicated on each corresponding bar.

radical that affects the PVP molecule [45,46], see Fig. 6. The C—H bond in the $CH_2$ group adjacent to nitrogen is the weakest bond in lactams and N-alkylamides [47], therefore generation of a macroradical occurs on this group in PVP monomer. There are two potential sites for radical formation – one C atom in the lactam ring (4) and one C atom in the polymer chain (5) (Fig. 6). Abstraction of H atoms from the N adjacent carbon is achieved by the ketyl radicals. An aliphatic carbon-centered radical is formed (reaction (I) in Fig. 6) [45] as well as an alkyl radical which in the presence of oxygen is immediately oxidized to a peroxy radical transforming subsequently into pyrrolidone hydroperoxide (reaction (II) in Fig. 6) [46]. Ultimately, all the radicals that are generated recombine with each other to form a polymer net based on different cross-linking bonds (Fig. 6). The resulting covalent bonds increase the crowding of the molecules and shorten the distance between the atoms, thus tightening the polymer net. Such action makes the tensile strength and elongation at break of cross-linked fibers greater than that of non-cross-linked fibers. However, the longer the cross-linking time is, the more free radicals and more bonds in the polymer mesh are formed. Its elasticity decreases, and the more and more dense structure becomes prone to breaking.

The mechanical properties of fibrous mats change when the fibers are electrospun with the addition of microspheres. In the case of PCL microspheres, a decrease in their strength can be noticed compared to pure PVP fibers (blue bars, Fig. 5) – both for the content of microspheres of 10 mg/mL and 20 mg/mL, but the addition of a larger amount improves the mechanical properties, especially for a short cross-linking time (2 × 5 min). The addition of PES microspheres increases the mechanical strength of mats in relation to both pure PVP fibers and those with the addition of PCL – again especially for a short cross-linking time. A similar phenomenon of increasing the mechanical strength of fibers after adding microspheres was previously noted by Balzamo et al. [20].

Different properties of fibrous mats with the addition of PCL and PES may result from differences in the size of the microspheres. PES microspheres have more than twice smaller diameters than PCL ones (14.38 ± 6.28 μm for PCL and 6.20 ± 2.43 μm for PES) [35]. As a result, in the case of PCL microspheres in the fibrous net, there are more places where one microsphere is at the interface of two (or more) fibers, which obviously weakens the entire structure.

The microspheres are firmly attached to the fibers which can be observed in SEM pictures (Fig. 4E–F). During the strength tests and application of stress, the fibers elongate, change diameter, and align along the direction of the force while the microspheres maintain their shape and resist the tensile stress by holding the fibers. In addition, there is a high probability that during cross-linking with ultraviolet light, in the structure of microsphere-forming polymers free radicals may be formed too – both PCL and PES may undergo such a reaction [48,49]. These radicals can increase the strength of the polymer net by formation of the bonds between the fibers and the microspheres. This results in a higher stress required to rupture modified fibers.

Extending the cross-linking time of fibers makes them much less flexible (which is reflected in the elongation at break parameter, Fig. 5B), and thus much less mechanically resistant. There are no significant differences between the strength of UV-cross-linked fibers for 2 × 15 min and 2 × 60 min. Due to this, it was decided to reject the 2 × 60 min UV-cross-linked samples in the course of further research.

### 3.4. Rhodamine immobilization in the mats

In Fig. 7 a bar graph is presented showing the equilibrium concentration of rhodamine in solution after the release from PVP fibers UV-cross-linked for 2 × 5 and 2 × 15 min depending on the content of microspheres in the fibers and type of microspheres.

Fig. 7 shows that the addition of microspheres increases the drug capacity of the electrospun fibrous mat. Increased content of PCL microspheres from 10 mg/mL to 20 mg/mL increases the concentration of released rhodamine from about 0.0017 mg/mL to 0.0024 mg/mL for a 2 × 5 min sample. The addition of PES microspheres in the amount of 20 mg/mL does not cause the same increase in the capacity of the mat for the drug as the addition of PCL microspheres in this amount for the 2 × 5 min sample. This is due to the greater interface surface area of the PCL-microsphere-loaded fibers (10.20 ± 0.40 $m^2/g$) which is almost two times larger than the surface of PES-microsphere-loaded ones (5.17 ± 0.10 $m^2/g$), see Table 1. Fig. 7 also shows that the extended cross-linking time reduces the amount of rhodamine released from the microsphere-loaded fibers, confirming that UV radiation may have an effect on the marker content of the system. The process of UV-cross-linking with benzophenone resulted in the loss of the pink color of mats visible with the unaided eye, which was reflected in the determination of the amount of released rhodamine using the spectrophometric method.

In the current study, the diameters of the microspheres are significantly larger in comparison to the diameters of the fibers (up to 20 times), which serves as a contributing factor to the augmented capacity of the system for the active ingredient. Other systems, as previously documented in the literature, have employed microspheres with diameters that range from

1–3 μm [31,34], 36–39 μm [32] or 10–100 μm [33], however, none of the studies has evaluated the extent to which the total volume of the system has increased. The capacity of the proposed system for the active substance can be controlled by selecting the type, size and concentration of microspheres. The amount of the active substance should be selected depending on its specific therapeutic dose and individual needs.

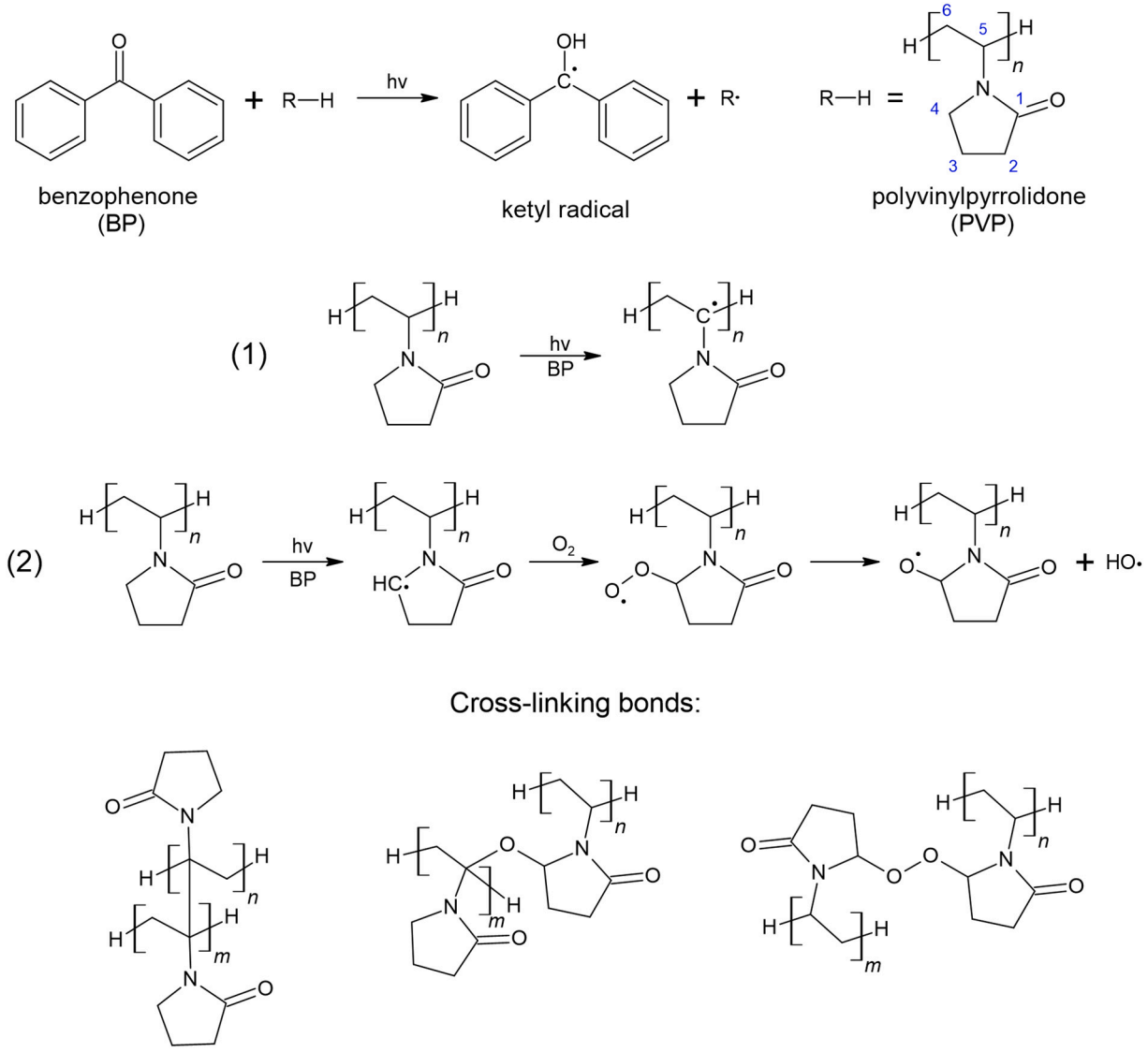


**Fig. 6.** Reaction mechanism of the formation of cross-linking bonds of PVP. Photocatalytic formation of free radicals and PVP hydroperoxide species [45,46].

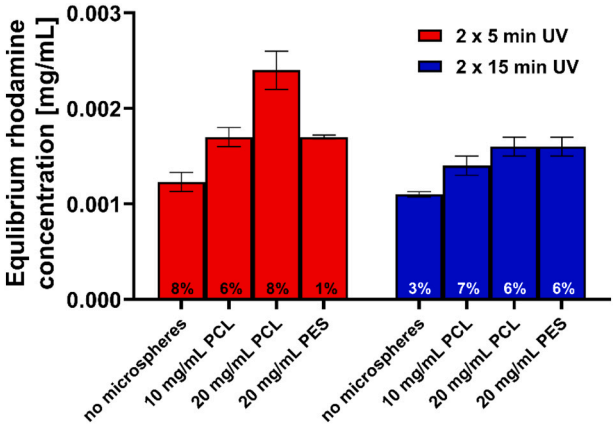


**Fig. 7.** Equilibrium rhodamine concentration after 4 h of release from UV-cross-linked PVP fibers with the addition of substance-loaded microspheres depending on the quantity and type of microspheres and cross-linking time. The coefficient of variations of equilibrium rhodamine concentration is indicated on each corresponding bar.

**Table 1**
Specific surface of microsphere-loaded fibers *A* and the transport coefficient *h* depending on the type of microspheres and the cross-linking time of the mats.

| Sample | Coefficient of determination $R^2$ [−] | BET surface area *A* [$m^2$/g] | Transport coefficient $h \times 10^{-6}$ [cm/min] ± VC [%] |
|---|---|---|---|
| PVP_PCL/ Rod_2 × 5 | 0.9812 | 10.20 ± 0.40 | 2.32 ± 17 % |
| PVP_PCL/ Rod_2 × 15 | 0.9513 | 4.36 ± 0.19 | 6.43 ± 8 % |
| PVP_PES/ Rod_2 × 5 | 0.9367 | 5.17 ± 0.10 | 26.58 ± 11 % |
| PVP_PES/ Rod_2 × 15 | 0.9031 | 4.77 ± 0.09 | 5.69 ± 18 % |

### 3.5. Kinetics of rhodamine release

The controlled substance release is an important ability of the fibrous mat from the point of view of its potential use as a drug delivery system. The next stage of research within the framework of the present work focuses on investigating rhodamine release profiles from the designed electrospun UV-cross-linked polyvinylpyrrolidone fibers modified with

polycaprolactone/polyethersulfone with a specific focus on the kinetics of the release process during the first stage. Fig. 8 contains the plots showing the rhodamine release profiles from different fibrous mats over the period of 24 h. The curves are divided into three groups differing in colors, red for samples of rhodamine-loaded PVP fibers without microspheres, blue for PCL/Rod-loaded fibers and green for PES/Rod-loaded ones. The bar plot in Fig. 8 the values of transport coefficient *h* determined with *OriginLab* software using Eq. (4).

For UV-cross-linked PVP electrospun fibers, the burst effect occurring at the beginning of the release process is clearly visible in the rhodamine release profiles of PVP_Rod mats without the addition of microspheres (Fig. 8A). It is characterized by a very rapid increase in the marker concentration above the equilibrium concentration reached later. For the 2 × 5 min UV-cross-linked fibers, the rhodamine concentration after burst release is about 0.33 mg/mL, and then it drops to 0.20 mg/mL in the equilibrium state. In the case of a 2 × 15 UV-cross-linked sample, this difference is smaller, and the mentioned concentrations are 0.14 mg/mL and 0.9 mg/mL, respectively. The decrease in this concentration is certainly not related to the adsorption of rhodamine in the measuring system, because appropriate tests were carried out before starting the experiments and such a problem was eliminated. This decrease may be the result of the cross-linking blocking the rapid release of substances from the fibers. In a highly cross-linked fibrous mat, the distances between the polymer chains are smaller according to the cross-linking mechanism described before. In such a case, the relatively large rhodamine molecule (591.06 g/mol) may have difficulty diffusing outward from the densely packed polymer net. The reduction of burst effect from cross-linked fibrous mats was also observed by Zhang et al. [50] who electrospun of polyvinyl alcohol/collagen fibers. They eliminated the burst effect of salicylic acid release after 4 h of UV-cross-linking.

Burst release occurs in the first 30 min of the experiment and the close-up of this period is shown in Fig. 8C. Fitting the model of the straight line to the experimental points allows one to obtain the value of the slopes, which explicitly determines the speed of the ongoing process. For fibers without microspheres cross-linked longer, the burst effect is lower, the slope of the line is more than twice as low (α = 0.649 for PVP_Rod_2 × 5 and α = 0.296 for PVP_Rod_2 × 15). The modification of the fibers by the addition of microspheres resulted in a slower release of

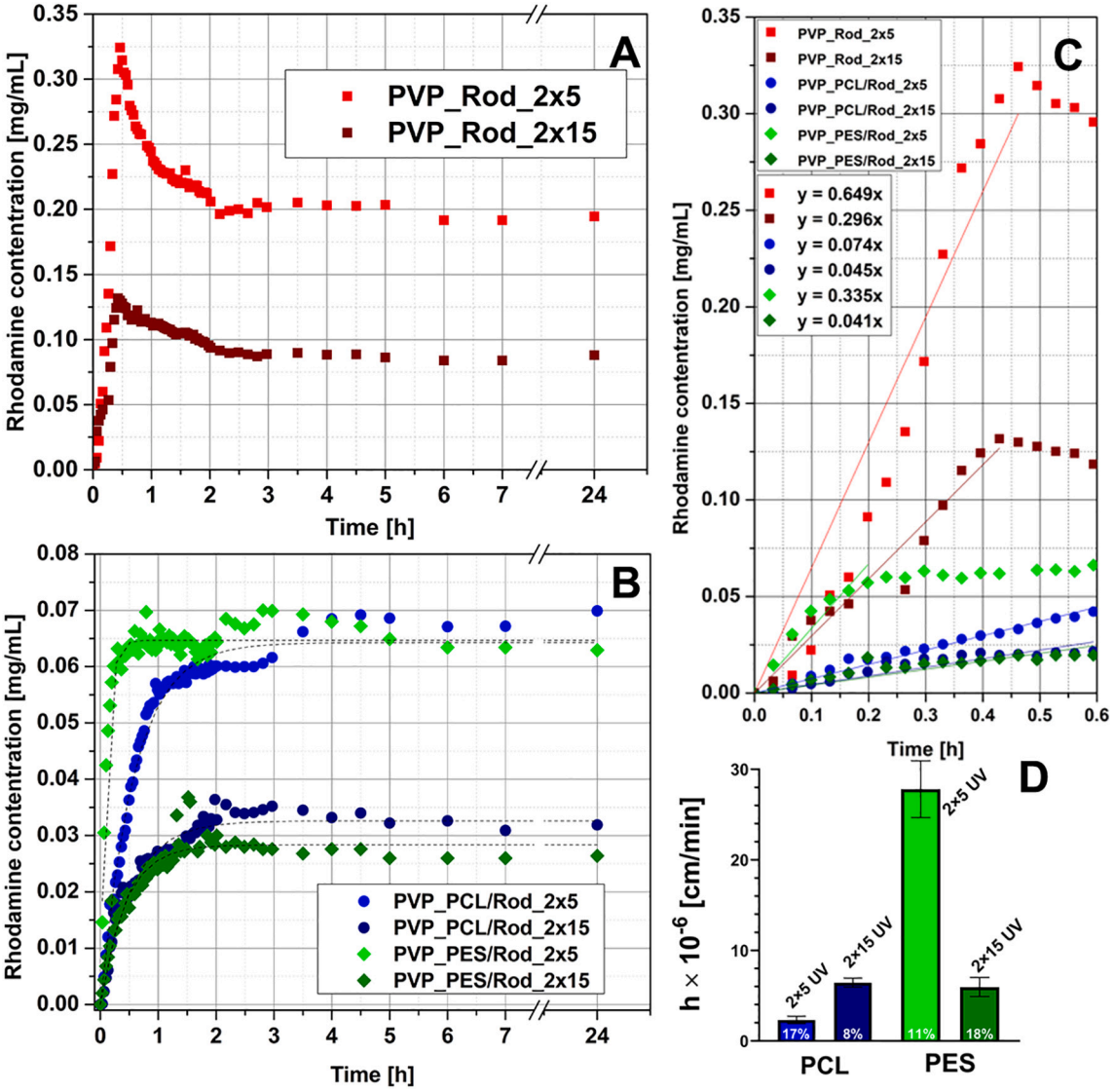


**Fig. 8.** Rhodamine release profiles from UV-cross-linked PVP fibrous mats. (A) Full release profile from fibers without microspheres – PVP_Rod (rhodamine encapsulated directly in the fibers). (B) Full release profile from fibers with the addition of rhodamine-loaded PCL (PVP_PCL/Rod) or PES (PVP_PES/Rod) microspheres with model curves fitted to experimental. (C) Close-up of the first release period of the first 30 min from all samples with linear model fit with the formula $y = \alpha x$, the equations of fitted functions are given in the graph. (D) The values of the transport coefficient *h* for UV-cross-linked PVP fibrous mats with the PCL or PES microspheres depending on the cross-linking time. The coefficient of variations of *h* are indicated on each corresponding bar as well as in Table 1.

the substance in the first period. The α coefficients for PCL-microsphere-loaded fibers (blue points in Fig. 8C) are an order of magnitude lower than those for mats without microspheres. In this case also a longer cross-linking time causes an almost two-fold decrease in the substance release rate (α = 0.074 for PVP_PCL/Rod_2 × 5 and α = 0.045 for PVP_PCL/Rod_2 × 15). A similar phenomenon is observed for fibers containing PES microspheres. Both for the cross-linking time of 2 × 5 min and 2 × 15 min, the slope coefficients of the straight line are lower than for analogous nonwovens without microspheres. On the other hand, increase of the cross-linking time causes an eightfold decrease in the release rate (α = 0.335 for PVP_PES/Rod_2 × 5 and α = 0.041 for PVP_PES/Rod_2 × 15).

No burst effect was observed in the rhodamine release profiles from mats with microspheres (Fig. 8B) – it was effectively eliminated by using fibers modified in the proposed manner. The release profiles of such microsphere-loaded fibers show that it proceeds in two steps in some cases. This may be due to the fact that the fibers swell slightly when submerged in water, which was previously observed as an increase in their diameter during degradation studies (Fig. 3). Moreover, the fiber/microsphere structure is specific. Rhodamine is not only enclosed in microspheres – at the stage of preparing the mixture for electrospinning (Fig. 1B) some of the rhodamine penetrates from the microspheres into the PVP solution. Thus, it is first released from the polymer shell covering the microsphere, and only later the substance enclosed inside the microspheres reaches the solution.

In previously reported studies [31–33], drug-loaded microspheres were incorporated into polymer fiber networks at different stages of the manufacturing process ("sandwich" system). Each of these systems was designed for different potential applications. Initial measurements of the concentration of the substance in solution were carried out only after 3 to 4 h, and, moreover, the authors did not take samples very often, which is necessary to accurately determine the kinetics of the release profile of the active substance.

Xu et al. [34] developed a biodegradable system for the delivery of two drugs by suspension electrospinning, in which the release of the active ingredient is based on a biodegradation process. The authors found that the burst effect was eliminated by coating the microspheres with an outer layer of a fibrous polymer, given that microsphere diameters were comparable to the fiber diameters. However, the results presented in the publication do not clearly indicate the elimination of the burst effect, as the authors included the results of measurements carried out only after 1 h, without thoroughly investigating the kinetics of the substance release during the first stage of the process.

On the other hand, S. Park et al. [51] showed that core/shell fibers with monolithic PCL coating, compared to PVP/PCL coated fibers, showed a reduced burst effect followed by prolonged sustained release of the drug substance. Da Silva et al. [52] found that monolithic PVA fibers showed burst release, while core-shell fibers composed of PLA and PVA were characterized by controlled albumin release. In the case of presented system – fibrous mats modified with PCL/PES microspheres with diameters up to 20 times larger than the fiber diameters – the burst effect does not occur either. It leads to supposition that it exhibit a structure similar to that observed in above studies – microspheres are covered with an outer PVP layer which delays the release of the substance. As such, the solution electrospinning technique employed in this study can be considered an alternative to more complex core/shell electrospinning systems, showcasing its potential as a competitive method in the field. However, further characterization of the structure of the fabricated systems would be necessary to confirm these conclusions.

Due to the absence of burst effect, the rhodamine release curves from mats with microspheres can be described by an exponential function (Eq. (4)). Relevant calculations were carried out, and an exemplary result is shown in Fig. SI2 (*Supporting Information*), the table with the results of the mathematical analysis is included. The values of the coefficients of determination $R^2$ for each sample are above 0.9 (Table 1), the fit is therefore very good. For each case, parameter $b$ was determined from Eq. (4), and then using Eq. (6), the transport coefficient $h$ was determined for each case. The results are shown in the Table 1 together with BET surface area and at the bar graph in Fig. 8D.

The value of the coefficient $h$ obtained for the PVP/PES_Rod_2 × 5 min mats is the greatest ($26.58 \times 10^{-6}$ cm/min ± 11 %) and clearly exceeds the others by more than four times. For both samples UV-cross-linked for 2 × 15 min (PVP_PCL/Rod_2 × 15 and PVP_PES/Rod_2 × 15) the $h$ values are similar (respectively, $6.43 \times 10^{-6}$ cm/min ± 8 % and $5.69 \times 10^{-6}$ cm/min ± 18 %). The PVP_PCL/Rod_2 × 5 sample differs from the others ($h = 2.32 \times 10^{-6}$ cm/min ± 17 %) which is due to the more than twice the interface surface area of this sample compared to the others (the value of this surface is in the denominator in the Eq. (6)). The explanation of such a large surface development in this specific case requires further research.

The applied method of mathematical description of substance release was previously proposed by Grzeczkowicz et al. [42] to model kinetics of the release of vitamin B12 from microcapsules using the transport coefficients $h$. For synthetic porous membranes, the value of $h$ was three orders of magnitude greater than those observed in this work for UV-cross-linked microsphere-loaded fibers, although the materials tested in the cited work had a much greater thickness (182–272 μm) compared to the fibers and microspheres (1–15 μm). The release rate was mainly influenced by the porous structure of membranes which the UV-cross-linked PVP fibers do not have. A marked slowdown in the substance release is beneficial from the point of view of drug delivery systems, and it occurs even for a marker with a molecular weight twice as low (rhodamine: 591 g/mol, vitamin B12: 1355 g/mol). Besides, Grzeczkowicz et al. approximated the interface by the size of the total geometric area of all microspheres and no real specific surface area was used.

### 3.6. Antibacterial properties

UV-cross-linked microsphere-loaded fibrous PVP mats with enhanced capacity for active substance may be useful e.g. for wound dressing applications regarding the need to maintain sterility at the wound site. In that frame, we loaded such mats with ampicillin and performed an agar diffusion inhibitory growth test to characterize their antimicrobial activity. The tests were carried out with the sample 2 × 5 min and 2 × 15 min samples with drug-loaded PCL or PES microspheres. Each sample was deposited on the surface of nutrient agar plate previously inoculated with *E. coli* or *S. aureus* at a concentration of $10^8$ CFU/mL and incubated for 24 h. Fig. 9 illustrates the results of the antibacterial properties study.

The studies presented in this work (Fig. 9) show that mats modified with both PCL and PES microspheres exhibit antibacterial activity, but it is much higher when exposed to *S. aureus* bacteria. Moreover, fibers with PCL microspheres have stronger bactericidal effect – a much larger clear zone is observed (Fig. 9B). On the other hand, prolonged crosslinking time results in a reduced clear zone, especially for fibers with PES microspheres. Both of these observations are consistent with the results of the research on the capacity of the systems for the active substance (Fig. 7). UV-treated PVP fibers without microspheres and without drug show no bactericidal activity, which confirms that no toxic substances are formed during UV-cross-linking and that the benzophenone used is also non-toxic. The bar chart in Fig. 9C presents the results of the inhibitory zone area measurements obtained from images of Petri dishes, in which the antibacterial properties of the modified mats were tested. The results are based on three replicate experiments and are presented with the mean values, standard deviation and coefficient of variation being depicted. The results of the antibacterial activity, as observed in the photos, are reflected in the chart. A trend can be identified, wherein an increase in the duration of cross-linking results in a decrease in the antibacterial activity of the mats. There is a slight difference in the activity between PCL and PES-loaded mats. However, the sample containing PES microspheres and cross-linked for 2 × 15 min (for both *E. coli* and *S. aureus*) deviates notably from the others. Further

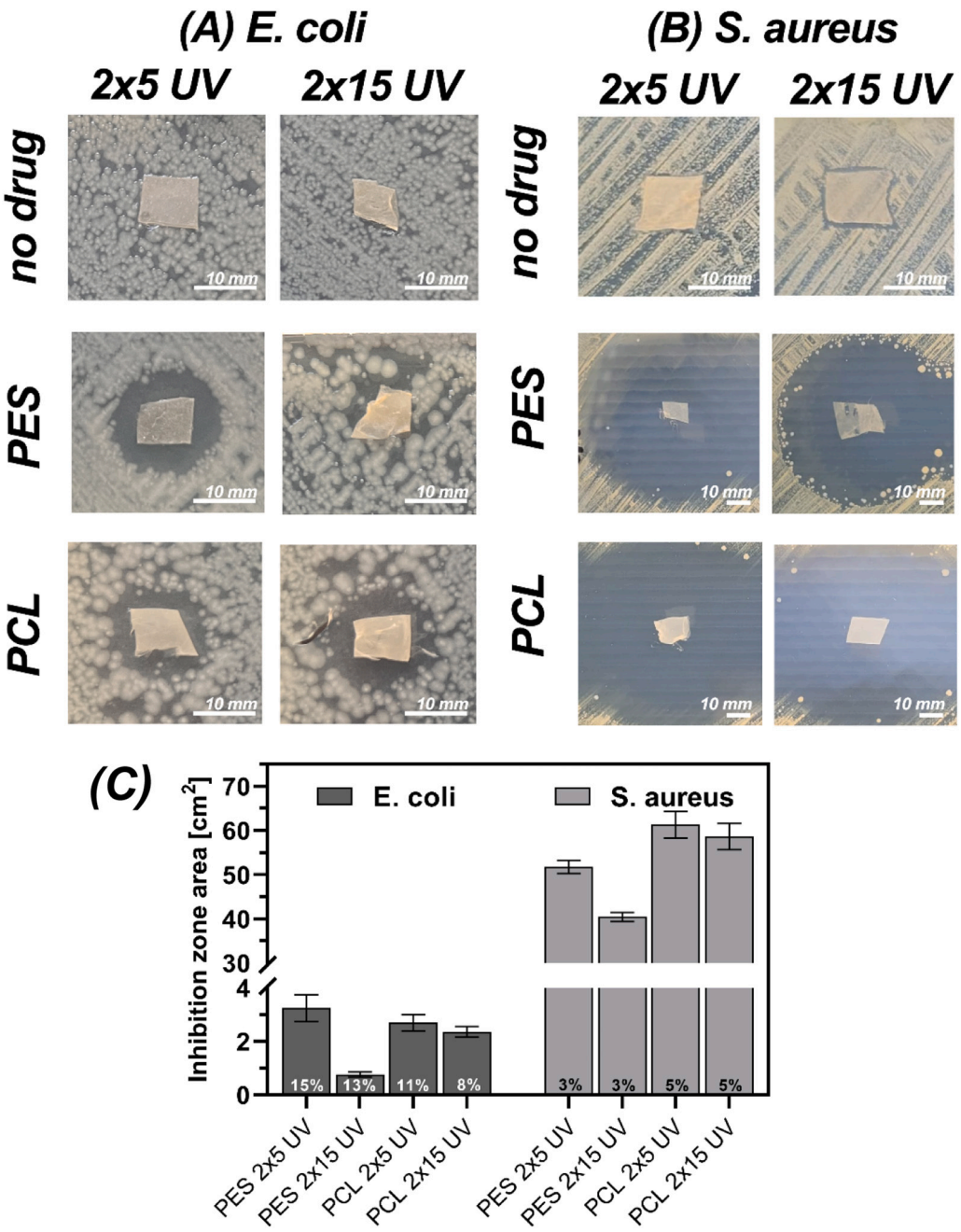


**Fig. 9.** Bacteriostatic tests of UV-cross-linked PVP fibrous mats with ampicillin-loaded microspheres on nutrient agar plates covered with (A) *E. coli* and (B) *S. aureus* biofilms after 24 h of material treatment. (C) Bar chart showing average inhibition zone areas [$cm^2$] based on images of Petri dishes from three test replicates. The coefficient of variations is indicated on each corresponding bar.

research is necessary to fully understand this phenomenon. Additionally, it can be noted that the zones of inhibited growth for *S. aureus* are significantly larger in comparison to those observed for *E. coli*.

Li et al. [31] report that the systems they developed (electrospun silk/PCL/PVA fibers with drug-filled silk/chitosan microspheres applied to their surface) showed excellent antimicrobial activity with 93.18 % and 97.15 % inhibition of *E. coli* and *S. aureus*, respectively, however, they used a different method to determine the antibacterial properties of fibrous mats. A similar test using nutrient agar plates coated with bacteria was conducted by Nagarajan et al. [53], who investigated the antibacterial properties of chemically crosslinked gelatin fibers loaded with chlorhexidine acetate. They obtained inhibition zone diameters of $2.7 \pm 0.3$ $cm^2$ for *E. coli* bacteria, similar to those obtained in presented study. They also tested Gram-positive bacteria, *Staphylococcus epidermidis* (the same genus as in this work) and they report an inhibition zone diameter of $2.7 \pm 0.3$ $cm^2$, 20 times less than in the case of ampicillin-loaded microsphere-modified fibrous mats, probably due to a stronger activity of ampicillin against the microorganisms. The reported bactericidal activity of this loaded electrospun mat is quite promising, as it demonstrated the ability to remove a significant number of colony-forming units within a small area, as determined by standardized contact tests (minimum $10^7$ CFU of bacteria killed which corresponds to an area of 0.5 $cm^2$) [54]. The tests conducted evidenced that the integrity of the drug had not been affected during microsphere preparation and electrospinning process. Hence, the proposed fibrous mats could serve as controlled drug delivery systems.

## 4. Conclusions

All the assumed goals of the work have been achieved. The application of the microsphere suspension electrospinning method, incorporating the unconventional utilization of pulsed voltage, made it possible to manufacture electrospun PVP fibers modified with drug-loaded PCL (or PES) microspheres of a structure meeting a set of specific requirements. As expected, the addition of microspheres to electrospun fibers increases the capacity of the entire system for the drug and eliminates the undesirable burst effect. In addition, it was found that the amount and type of microspheres used in the electrospun mats notably affect their mechanical properties, increasing their strength, and upgrade the release profile of the active substance. As assumed, UV-crosslinking of modified electrospun mats (using benzophenone as photoinitiator) results in water- and ethanol-insoluble fibers, making them more flexible in terms of potential applications. It was also found that the time of UV-crosslinking remarkably impacts the properties of such mats, including degradation rate, mechanical strength and transport properties. Both electrospun mats with PCL and PES microspheres exhibit good antibacterial properties. The presented method of fiber mat manufacturing is highly versatile – allowing for a wide range of modifications to be made with respect to potential applications, such as the size and porosity of microspheres, the polymers used, the concentration of the cross-linking agent, and the duration of cross-linking, etc. Therefore, it can be concluded that the presented electrospun mat based on UV-crosslinked polyvinylpyrrolidone (PVP) fibers modified with polycaprolactone (PCL) or polyethersulfone (PES) microspheres demonstrates great potential as a drug delivery system.

## CRediT authorship contribution statement

**Adam Mirek:** Conceptualization, Methodology, Formal analysis, Investigation, Data curation, Writing – original draft, Writing – review & editing, Visualization. **Marcin Grzeczkowicz:** Conceptualization, Methodology, Validation, Formal analysis, Writing – review & editing. **Habib Belaid:** Methodology, Investigation, Writing – review & editing, Visualization. **Aleksandra Bartkowiak:** Conceptualization, Validation, Writing – original draft, Writing – review & editing. **Fanny Barranger:** Investigation, Visualization. **Mahmoud Abid:** Investigation. **Monika Wasyłeczko:** Methodology, Investigation, Visualization. **Maksym Pogorielov:** Methodology, Validation, Resources. **Mikhael Bechelany:** Conceptualization, Methodology, Validation, Resources, Writing – review & editing. **Dorota Lewińska:** Conceptualization, Methodology, Validation, Resources, Writing – original draft, Writing – review & editing, Supervision.

## Conflict of interest

All authors declare that they have no conflicts of interest.

## Data availability

Data will be made available on request.

## Acknowledgments

This project was supported by European Social Fund [POWR.03.02.00-00-1028/17-00] as part of the POWER Och!Dok program. AM would like to thank Campus France for the funding through a French Government Scholarship. Authors acknowledge the financial support of project H2020-MSCA-RISE-2017, “Novel 1D photonic metal oxide nanostructures for early stage cancer detection” (Project number: 778157).

## Appendix A. Supplementary data

Supplementary data to this article can be found online at https://doi.org/10.1016/j.bioadv.2023.213330.

## References

[1] C.A. Martínez-Pérez, Electrospinning: a promising technique for drug delivery systems, Rev. Adv. Mater. Sci. 59 (2020) 441–454.
[2] S.C. Kundu, N. Bhardwaj, Electrospinning: a fascinating fiber fabrication technique, Biotechnol. Adv. 28 (2010) 325–347.
[3] A. Memic, T. Abudula, H.S. Mohammed, K. Joshi Navare, T. Colombani, S. A. Bencherif, Latest progress in electrospun nanofibers for wound healing applications, ACS Appl. Bio Mater. 2 (3) (2019) 952–969.
[4] B. Guo, P.X. Ma, Synthetic biodegradable functional polymers for tissue engineering: a brief review, Sci. China Chem. 57 (2014) 490–500.
[5] M. Afrashi, D. Semnani, Z. Talebi, P. Dehghan, M. Maherolnaghsh, Comparing the drug loading and release of silica aerogel and PVA nano fibers, J. Non-Cryst. Solids 503–504 (2019) 186–193.
[6] Y. Liu, X. Chen, Y. Liu, Y. Gao, P. Liu, Electrospun coaxial fibers to optimize the release of poorly water-soluble drug, Polymers 14 (2022) 469.
[7] A. Domokos, A. Balogh, D. Denes, G. Nyerges, L. Zodi, B. Farkas, G. Marosi, Z. Nagy, Continuous manufacturing of orally dissolving webs containing a poorly soluble drug via electrospinning, Eur. J. Pharm. Sci. 124 (2018) 71–79.
[8] B.M. Maciejewska, J.K. Wychowaniec, M. Woźniak-Budych, Ł. Popenda, A. Warowicka, K. Golba, S. Jurga, UV cross-linked polyvinylpyrrolidone electrospun fibres as antibacterial surfaces, Sci. Technol. Adv. Mater. 20 (1) (2019) 979–991.
[9] Z. Wei, C. Xiong, Z. Liu, X. Wang, S. Long, J. Yang, Release characteristics and processing-structure-performance relationship of electro-spinning curcumin-loaded polyethersulfone based porous ultrafine fibers, J. Biomater. Sci. Polym. Ed. 29 (15) (2018) 1825–1838.
[10] Z. Wei, E. Liu, H. Li, Z. Wei, Z. Lv, Release characteristics of different diameter ultrafine fibers as antibacterial materials, J. Innov. Opt. Health Sci. 14 (2) (2021), 2041005.
[11] W. Chen, A. Palazzo, W.E. Hennink, R.J. Kok, Effect of particle size on drug loading and release kinetics of gefitinib-loaded PLGA microspheres, Mol. Pharm. 14 (2) (2017) 459–467.
[12] J. Yoo, Y.-Y. Won, Phenomenology of the initial burst release of drugs from PLGA microparticles, ACS Biomater. Sci. Eng. 6 (11) (2020) 6053–6062.
[13] J. Wu, Z. Zhang, J. Gu, W. Zhou, X. Liang, G. Zhou, C. Han, S. Xu, Y. Liu, Mechanism of a long-term controlled drug release system based on simple blended electrospun fibers, J. Control. Release 320 (2020) 337–346.
[14] X. Huang, C.S. Brazel, On the importance and mechanisms of burst release in matrix-controlled drug delivery systems, J. Control. Release 73 (2–3) (2001) 121–136.
[15] E.J. Torres-Martinez, J.M. Cornejo Bravo, A. Serrano Medina, G.L. Perez Gonzalez, L.J. Villarreal Gomez, A summary of electrospun nanofibers as drug delivery system: drugs loaded and biopolymers used as matrices, Curr. Drug Deliv. 15 (2018) 1360–1374.
[16] J. Xiong, Y. Liu, A. Li, L. Wei, L. Wang, X. Qin, J. Yu, Mass production of high-quality nanofibers via constructing pre-Taylor cones with high curvature on needleless electrospinning, Mater. Des. 197 (2021), 109247.
[17] J.M. Ameer, A.K. PR, N. Kasoju, Strategies to tune electrospun scaffold porosity for effective cell response in tissue engineering, J. Funct. Biomater. 10 (2019) 30.
[18] S. Omer, L. Forgach, R. Zelko, I. Sebe, Scale-up of electrospinning: market overview of products and devices for pharmaceutical and biomedical purposes, Pharmaceutics 13 (2021) 286.
[19] S.C. Chen, X.B. Huang, X.M. Cai, J. Lu, J. Yuan, J. Shen, The influence of fiber diameter on electrospun polu(lactic acid) on drug delivery, Fibers Polym. 13 (9) (2012) 1120–1125.
[20] G. Balzamo, X. Zhang, W.A. Bosbach, E. Mele, In-situ formation of polyvinylidene fluoride microspheres within polycaprolactone electrospun mats, Polymer 186 (2020), 122087.
[21] T. Kowalczyk, Functional micro- and nanofibers obtained by nonwoven post-modification, Polymers 12 (5) (2020) 1087.
[22] K. Ghosal, R. Augustine, A. Zaszczynska, M. Barman, A. Jain, A. Hasan, N. Kalarikkal, P. Sajkiewicz, S. Thomas, Novel drug delivery systems based on triaxial electrospinning based nanofibers, React. Funct. Polym. 163 (2021), 104895.
[23] J. Yang, K. Wang, D.-G. Yu, Y. Yang, S.W.A. Bligh, G.R. Williams, Electrospun Janus nanofibers loaded with a drug and inorganic nanoparticles as an effective antibacterial wound dressing, Mater. Sci. Eng. C 111 (2020), 110805.
[24] J. Wang, M. Windbergs, Controlled dual drug release by coaxial electrospun fibers – impact of the core fluid on drug encapsulation and release, Int. J. Pharm. 556 (2019) 363–371.
[25] A. Khan, K. Huang, M. Khalaji, F. Yu, X. Xie, T. Zhu, Y. Morsi, Z. Jinzhong, X. Mo, Multifunctional bioactive core-shell electrospun membrane capable to terminate inflammatory cycle and promote angiogenesis in diabetic wound, Bioact. Mater. 6 (9) (2021) 2783–2800.
[26] M. He, H. Jiang, R. Wang, Y. Xie, C. Zhao, Fabrication of metronidazole loaded polycaprolactone)/zein core/shell nanofiber membranes via coaxial electrospinning for guided tissue regeneration, J. Colloid Interface Sci. 490 (2016) 27–278.

[27] C. Zhang, F. Feng, H. Zhang, Emulsion electrospinning: fundamentals, food applications and prospects, Trends Food Sci. Technol. 80 (2018) 175–186.
[28] A.O. Basar, S. Castro, S. Torres-Giner, J.M. Lagaron, H. Turkoglu Sasmazel, Novel poly(ε-caprolactone)/gelatin wound dressings prepared by emulsion electrospinning with controlled release capacity of ketoprofen anti-inflammatory drug, Mater. Sci. Eng. C 81 (2017) 459–468.
[29] T. Shibata, N. Yoshimura, A. Kobayashi, T. Ito, K. Hara, K. Tahara, Emulsion-electrospun polyvinyl alcohol nanofibers as a solid dispersion system to improve solubility and control the release of probucol, a poorly water-soluble drug, J. Drug Deliv. Sci. Technol. 67 (2022), 102953.
[30] J. Gao, B. Li, L. Wang, X. Huang, H. Xue, Flexible membranes with a hierarchical nanofiber/microsphere structure for oil adsorption and oil/water separation, J. Ind. Eng. Chem. 68 (2018) 416–424.
[31] T.-T. Li, L. Sun, Y. Zhong, H.-K. Peng, H.-T. Ren, Y. Zhang, J.-H. Lin, C.-W. Lou, Silk fibroin/polycaprolactone-polyvinyl alcohol directional moisture transport composite film loaded with antibacterial drug-loading microspheres for wound dressing materials, Int. J. Biol. Macromol. 207 (2022) 580–591.
[32] P.S. Gungor-Ozkerim, T. Balkan, G.T. Kose, A.S. Sarac, F.N. Kok, Incorporation of growth factor loaded microspheres into polymeric electrospun nanofibers for tissue engineering applications, J. Biomed. Mater. Res. 102 (6) (2014) 1897–1908.
[33] N. Nagiah, G. Ramanathan, L. Sobhana, U.T. Sivagnanam, N.T. Srinivasan, Poly (vinyl alcohol) microspheres sandwiched poly (3-hydroxybutyric acid) electrospun fibrous scaffold for tissue engineering and drug delivery, Int. J. Polym. Mater. Polym. Biomater. 63 (11) (2014) 583–585.
[34] J. Xu, Y. Jiao, X. Shao, C. Zhou, C. Zhou, Controlled dual release of hydrophobic and hydrophilic drugs from electrospun poly(L-lactic acid) fiber mats loaded with chitosan microspheres, Mater. Lett. 65 (17) (2011) 2800–2803.
[35] A. Mirek, M. Grzeczkowicz, C. Lamboux, S. Sayegh, M. Bechelany, D. Lewińska, Formation of disaggregated polymer microspheres by a novel method combining pulsed voltage electrospray and wet phase inversion techniques, Colloids Surf. A Physicochem. Eng. Asp. 129246 (2022).
[36] A. Mirek, P. Korycka, M. Grzeczkowicz, D. Lewińska, Polymer fibers electrospun using pulsed voltage, Mater. Des. 108106 (2019).
[37] K. Li, Y. Wang, G. Xie, J. Kang, H. He, K. Wang, Y. Liu, Solution electrospinning with a pulsed electric field, J. Appl. Polym. Sci. 135 (15) (2017) 46130.
[38] Inc. Allevi, Allevi Protocols: Cell-Bioink Mixing: Syringe Coupler Method [Online]. Available:, Allevi, 13 July 2022 https://www.allevi3d.com/cell-bioink-mixing-syringe-coupler-method/. (Accessed 16 August 2022).
[39] W. Chrzanowski, E. Ali, A. Neel, D. Andrew, J. Campbell, Effect of surface treatment on the bioactivity of nickel - titanium, Acta Biomater. 4 (6) (2008) 1969–1984.
[40] A.W. Hansen, L.T. Fuhr, L.M. Antonini, D.J. Villarinho, C.E. Bruno Marino, C. de Fraga Malfatti, The electrochemical behavior of the NiTi alloy in different simulated body fluids, Mater. Res. 18 (1) (2015) 184–190.
[41] D.F. Radcliffe, J.D.S. Gaylor, Sorption kinetics in haemoperfusion columns. Part I. Estimation of mass-transfer parameters, Med. Biol. Eng. Comput. 19 (1981) 617–627.
[42] M. Grzeczkowicz, D. Lewińska, A method for investigation transport properties of partly biodegradable spherical membranes using vitamin B12 as the marker, Desalin. Water Treat. 128 (2018) 170–178.
[43] M. Contardi, D. Kossyvaki, P. Picone, M. Summa, X. Guo, J.A. Heredia-Guerrero, I. S. Bayer, Electrospun polyvinylpyrrolidone (PVP) hydrogels containing hydroxycinnamic acid derivatives as potential wound dressings, Chem. Eng. J. 409 (2021), 128144.
[44] P. Korycka, A. Mirek, K. Kramek-Romanowska, M. Grzeczkowicz, D. Lewińska, Effect of electrospinning process variables on the size of polymer fibers and bead-on-string structures established with a 23 factorial design, Beilstein J. Nanotechnol. 9 (2018) 2466–2478.
[45] S.K. Christense, M.C. Chiappelli, R.C. Hayward, Gelation of copolymers with pendent benzophenone photo-cross-linkers, Macromolecules 45 (2012) 5237–5246.
[46] X. Zhu, P. Lu, W. Chen, J. Dong, Studies of UV crosslinked poly(N-vinylpyrrolidone) hydrogels by FTIR, Raman and solid-state NMR spectroscopies, Polymer 51 (2010) 3054–3063.
[47] L. Tang, D. Sallet, J. Lemaire, Photochemistry of polyundecanamides. 1. Mechanisms of photooxidation at short and long wavelengths, Macromolecules 15 (5) (1982) 1432–1437.
[48] M. Przybysz-Romatowska, J. Haponiuk, K. Formela, Poly(ε-caprolactone)/poly (lactic acid) blends compatibilized by peroxide initiators: comparison of two strategies, Polymers 12 (1) (2020) 228.
[49] N.A. Alenazi, M.A. Hussein, K.A. Alamry, A.M. Asiri, Modified polyether-sulfone membrane: a mini review, Des. Monomers Polym. 20 (1) (2017) 532–546.
[50] X. Zhang, K. Tang, X. Zheng, Electrospinning and crosslinking of COL/PVA nanofiber-microsphere containing salicylic acid for drug delivery, J. Bionic Eng. 13 (2016) 143–149.
[51] S. Park, M. Kim, K. Choi, J. Kim, S. Choi, Influence of shell compositions of solution blown PVP/PCL core-shell fibers on drug release and cell growth, RSC Adv. 8 (57) (2018) 32470–32480.
[52] T.N. da Silva, R.P. Gonçalves, C.L. Rocha, B.S. Archanjo, C.A.G. Barboza, M.B. R. Pierre, F. Reynaud, P.H. de Souza Picciani, Controlling burst effect with PLA/PVA coaxial electrospun scaffolds loaded with BMP-2 for bone guided regeneration, Mater. Sci. Eng. C Mater. Biol. Appl. 97 (2019) 62–612.
[53] S. Nagarajan, L. Soussan, M. Bechelany, C. Teyssier, V. Cavaillès, C. Pochat-Bohatier, S. Balme, Novel biocompatible electrospun gelatin fiber mats with antibiotic drug delivery properties, J. Mater. Chem. B 4 (6) (2016) 1134–1141.
[54] R. Gläser, J. Harder, H. Lange, J. Bartels, E. Christophers, J. Schröder, Antimicrobial psoriasin (S100A7) protects human skin from Escherichia coli infection, Nat. Immunol. 6 (1) (2005) 57–64.